Draft version July 24, 2024
Typeset using LaTeX **twocolumn** style in AASTeX631

LIGO SURF Interim Report 1

Charles F. A. Gibson [1,2] and Javier Roulet [1,3]

[1] *LIGO, California Institute of Technology, Pasadena, CA 91125, USA*
[2] *Department of Physics, Allegheny College, Meadville, Pennsylvania 16335, USA*
[3] *TAPIR, Walter Burke Institute for Theoretical Physics, California Institute of Technology, Pasadena, CA 91125, USA*

1. MOTIVATION

The properties of binary black hole (BBH) mergers observed from LIGO-Virgo-KAGRA detections can be informative of the formation channel of the system (e.g., Mandel & Farmer 2022). Two primary theories of the origin of BBHs exist. The first is that the systems were formed through stellar evolutionary channels. Namely, as a binary system between two intermediately massive stars evolved, both stars remained in orbit, with the resulting black holes (BHs) surviving the supernovae at the end of the stars' lives. Eventually, due to the emission of gravitational waves (GWs), the two coalesced into a single BH through a BH-BH merger.

Alternatively, the BBH system may have been formed dynamically. Through the gravitational interactions of stars and black holes in dense stellar environments such as globular clusters and galactic nuclei, scattering events can place two, previously unrelated BHs into orbit around each other. This would most likely be from a three-body interaction in which an intruding BH kicks a less massive companion from a the binary the other BH is in, yielding a BBH system.

One way to potentially differentiate between these two formation channels is through analyzing the precession of the orbit. The BHs in BBH systems that formed from binary stellar evolution likely have spins $\vec{S}$ that are aligned with the orbital angular momentum $\vec{L}$. This stems from the preferential alignment of stellar rotation axes with the $\vec{L}$ of the binary, initialized by the angular momentum in stellar nurseries. Additional complications such as kicks from the supernovae of companion stars in the binary may misalign spins. However, the details of these processes are still not well modeled, so approximations to the effects must be taken into account. The simplest of approximations neglect these kicks, claiming that $\vec{S}$ and $\vec{L}$ remain aligned through the entire binary evolution process through the BBH merger.

Conversely, dynamically formed BBH systems are much more likely to have isotropic spin distributions. Because there is no initial relationship between $\vec{S}$ and $\vec{L}$, the alignment of $\vec{S}$ and $\vec{L}$ is just as likely as the misalignment of the two vectors. This assumption leads to the prediction that the orbits of dynamically formed BBH systems are more likely to precess than the orbits of binary stellar evolution remnants.

By understanding the precession of a BBH system, information regarding the formation channel of the binary can be gleaned. In particular, analyzing the precession found in LIGO-Virgo data from O1, O2, and O3 can help inform predictions of the origins of known BBH merger candidates. With just under 100 candidates of BBH systems as of O3 (Abbott et al. 2023; Mehta et al. 2023; Nitz et al. 2023), statistical conclusions can begin to be made about the nature of BBH precession and, therefore, the origin of the BBH systems.

These conclusions may be especially useful in understanding the nature of binary evolution, dense stellar environments, and dynamical interactions.

Currently, there exists a parameter $\chi_{\rm p}$ that has been used to describe the precession of the orbit. However, claims of individual precessing candidates are controversial (Hannam et al. 2022; Payne et al. 2022). That is because this parameter is not necessarily very informative of the individual precession of a BBH system. The issues with $\chi_{\rm p}$ are described in detail in Section 2. This summer, we focus on defining a new parameter that can better constrain orbital precession of BBH systems. The progress made so far is detailed in Section 3, and the challenges encountered are outlined in Section 4

2. PROBLEM

The effective precession parameter currently used to describe the precession of a BBH system, $\chi_{\rm p}$, is defined as

$$\chi_{\rm p} = \max\left(\chi_1 \sin\theta_{S_1 L}, \frac{q(4q+3)}{3q+4}\chi_2 \sin\theta_{S_2 L}\right), \quad (1)$$

where χ_i is the dimensionless spin parameter of the BH i, q is the mass ratio m_2/m_1 (where $m_1 > m_2$), and $\theta_{S_i L}$ is the angle between the spin $\vec{S}$ of BH i and the orbital angular momentum $\vec{L}$ (Schmidt et al. 2015). When $\chi_{\rm p} =$

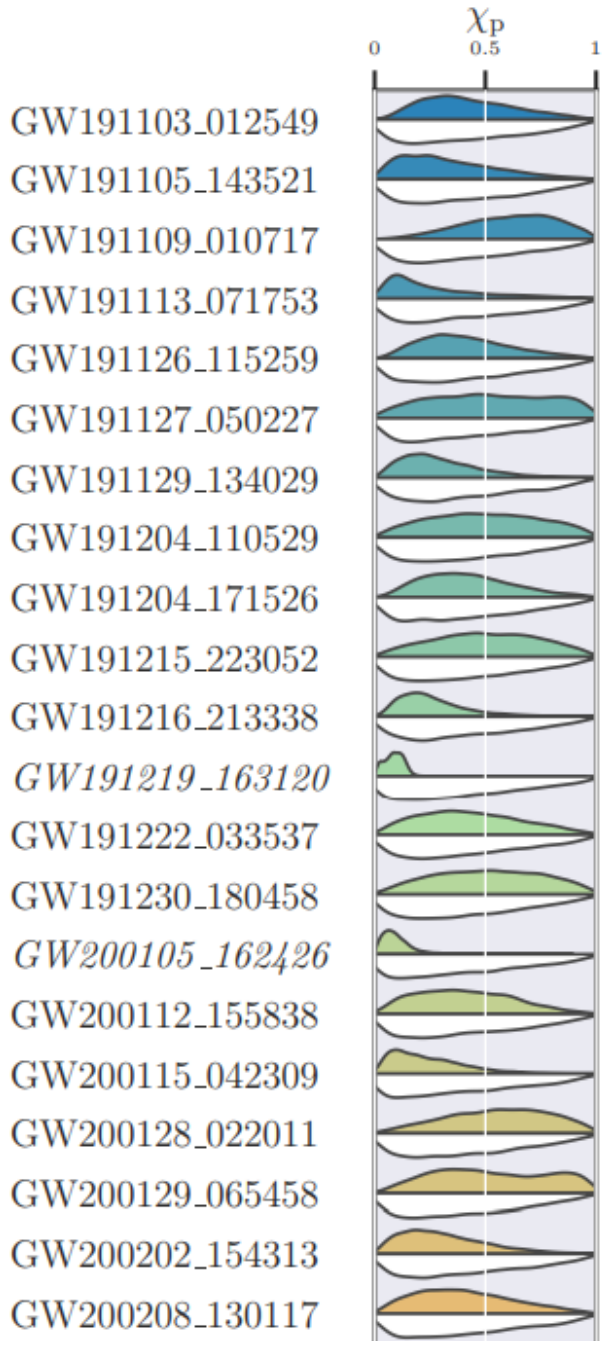

Figure 1. The χ_p distributions of several observations from Abbott et al. (2023). Note that most of the posteriors (upper curves) are very broad, only marginally differing from the prior distribution (lower curves). For the more localized posteriors, the localization only occurs at low values of χ_p where the peak in the prior occurs, and these events have high levels of uncertainty of astrophysical origin.

0, the system is not precessing, and when $\chi_p = 1$, the system is strongly precessing.

This parameter has two main issues that make it difficult to analyze precession: The first can be seen by the posterior distributions in Figure 1. Most of the posterior distributions for χ_p are very broad. A broad posterior distribution is not very informative on the true value associated with the data, as it makes it difficult to constrain the value to a reasonable range. The second is displayed by the prior distribution in Figure 1: the prior distribution of χ_p sharply approaches 0 as χ_p approaches 0. In mathematical terms, $\pi(\chi_p = 0) = 0$.

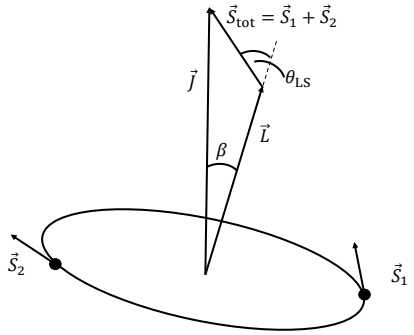

Figure 2. The geometry of a BBH system. The spins of each black hole are denoted by $\vec{S}_i$ (with the total spin $S_{tot} = \vec{S}_1 + \vec{S}_2$), the orbital angular momentum is expressed as $\vec{L}$, and the total angular momentum ($\vec{L} + \vec{S}_1 + \vec{S}_2$) is $\vec{J}$. θ_{LS} is the angle between $\vec{L}$ and $\vec{S}_{tot}$. β is the angle between $\vec{J}$ and $\vec{L}$.

The first issue makes χ_p a poor parameter statistically. The second issue fails to address a fundamental goal of the χ_p parameter: to reject the hypothesis that the spins are aligned. However, by initially assuming the spins are misaligned (as the probability of alignment is 0 in the prior in χ_p), the parameter fails to reject aligned spins. This is because the posterior distribution is defined as the prior distribution times the likelihood, so if the prior is 0 at a value, then the posterior will always be 0 at that value.

This summer, we aim to propose an alternative parameter that addresses these two issues. Namely, we want a parameter that has a well defined distribution and contains the true precession value, and we want a parameter that does not reject aligned spins in the prior.

3. ACCOMPLISHMENTS SO FAR

Using the geometry of the BBH merger outlined in Figure 2, two alternative parameters were initially selected based on the geometry of the system. First is θ_{LS}, the angle between the $\vec{L}$ and total spin $\vec{S}_{tot} = \vec{S}_1 + \vec{S}_2$. This angle provides a direct geometric understanding of the relationship between $\vec{S}_{tot}$ and $\vec{L}$, fundamentally relating to the orbital precession. The second is β, the angle between $\vec{L}$ and the total angular momentum $\vec{J} = \vec{S}_{tot} + \vec{L}$. β is especially promising because, as a precession indicator, it impacts the magnitude modu-

lations and phase evolution of the waveform (Fairhurst et al. 2020). Particularly, the parameter $b = \tan(\beta/2)$ is directly used to compute the waveform. However, unlike β, $\theta_{\rm LS}$, and $\chi_{\rm p}$, b has infinite bounds, making it more difficult to constrain a "maximum" precession. Regardless, $\theta_{\rm LS}$ and β share the same issue with $\chi_{\rm p}$ in the sense that their probability densities both tend towards zero when $\vec{S}$ and $\vec{L}$ are aligned. To combat this issue, we consider the cosine of the angles, $\cos\theta_{\rm LS}$ and $\cos\beta$. This coordinate shift to cosine is chosen because it yields a non-zero probability of aligned spins in the prior.

In order to measure how informative the three parameters ($\chi_{\rm p}$, $\cos\theta_{\rm LS}$, and $\cos\beta$) are, we needed to test them on known values. As the exact values of the main parameters from LIGO-Virgo-KAGRA sources are not known, we instead used synthetic data with posteriors formed from known injections. These injections were generated assuming an isotropic spin distribution. In other words, all true angles between $\vec{L}$ and $\vec{S}$ are equally likely in the synthetic data. We used roughly 3000 posteriors with known injection values in this data set that was used.[1]

Using the posterior distributions obtained from the injected samples, we constructed several functions to convert the raw (posterior) data into a posterior distribution of the parameters $\cos\beta$, $\cos\theta_{\rm LS}$, and $\chi_{\rm p}$. Initial examinations of the effectiveness of each parameter for a randomly selected case are shown in Figure 3.

However, in order to evaluate how informative each parameter is most effectively, we ran a statistical significance test, starting from the Neyman-Pearson Lemma. This is the strongest test for comparing two hypotheses, $\mathcal{H}_0$ and $\mathcal{H}_1$, against each other (in this case, having the $\vec{S}_{\rm tot}$ isotropically misaligned ($\mathcal{H}_0$) or aligned ($\mathcal{H}_1$) with $\vec{L}$). This test is defined the likelihood ratio of two hypotheses, expressed as

$$\Lambda = \frac{p(d \mid \mathcal{H}_1)}{p(d \mid \mathcal{H}_0)} \tag{2}$$

(Neyman & Pearson 1933). If the probability of $\mathcal{H}_1$ is greater than the probability of $\mathcal{H}_0$, the ratio is greater than 1. A threshold to eliminate the null hypothesis $\mathcal{H}_0$ can be set.

Each hypothesis can be a set of parameters that yield some result. For the 1-dimensional case,

$$\mathcal{H}_0 :\ \theta \sim \pi(\theta) \tag{3}$$
$$\mathcal{H}_1 :\ \theta = \theta_*. \tag{4}$$

[1] The injections and posterior distributions can be found at https://zenodo.org/records/10910135.

In other words, $\mathcal{H}_0$ is the initial estimate of the probability distribution isotropic spin alignment, and $\mathcal{H}_1$ is the value corresponding to $\vec{S}_{\rm tot}$ and $\vec{L}$ alignment.

Using the relationship between the likelihood $\mathcal{L}$, the posterior $\mathcal{P}$, the prior π, and the evidence $\mathcal{Z}$,

$$\mathcal{P} = \frac{\mathcal{L}\pi}{\mathcal{Z}} \tag{5}$$

and the definitions of $\mathcal{H}_0$ and $\mathcal{H}_1$, we can express the likelihood $p(d \mid \mathcal{H}_1)$ as

$$p(d \mid \mathcal{H}_1) = p(d \mid \theta_*) \tag{6}$$
$$p(d \mid \theta_*) = \mathcal{L} \tag{7}$$
$$\mathcal{L} = \frac{p(\theta_* \mid d, \mathcal{H}_0)\, p(d \mid \mathcal{H}_0)}{\pi(\theta_* \mid \mathcal{H}_0)}. \tag{8}$$

Plugging this into Equation (2), we get

$$\frac{p(\theta_* \mid d, \mathcal{H}_0)}{\pi(\theta_* \mid \mathcal{H}_0)}. \tag{9}$$

However, a BBH system is not 1-dimensional, as it is defined by many parameters. Although precession is not necessarily based on a single parameter, our goal is to find a single parameter that can provide significant information on the precession of the system. We can express θ as a multidimensional parameter that contains a single parameter x that preserves the relevant precession information and all other unrelated parameters θ' as

$$\theta = (x, \theta') \tag{10}$$

We can then define a new Hypothesis $\tilde{\mathcal{H}}_1$ that remains as close to $\mathcal{H}_1$ as possible while only being based on one parameter. We choose $\tilde{\mathcal{H}}_1$ to differ from $\mathcal{H}_0$ by only one parameter as this will allow us to test simplified population models that only consider very few BBH parameters at a time. Ideally, there should be a single value of $x = x_*$ that allows $\mathcal{H}_0$ to be the same as $\tilde{\mathcal{H}}_1$. That is, in an isotropic spin distribution ($\mathcal{H}_0$), there should be only one orientation of the vectors that gives aligned spins $\tilde{\mathcal{H}}_1$ (again, based on a single parameter).[2] This is expressed as

$$\pi(\theta' \mid x_*, \tilde{\mathcal{H}}_1) = \pi(\theta' \mid x_*, \mathcal{H}_0), \tag{11}$$

and thus,

$$\pi(\theta \mid \tilde{\mathcal{H}}_1) = \delta(x - x_*)\pi(\theta' \mid x_*, \mathcal{H}_0). \tag{12}$$

[2] This approximation does neglect some information. For example, if the two spins have vertical components of $\vec{S}$ that align with $\vec{L}$ but the horizontal components of their spins cancel, this simplification fails to identify the spin misalignment in the system.

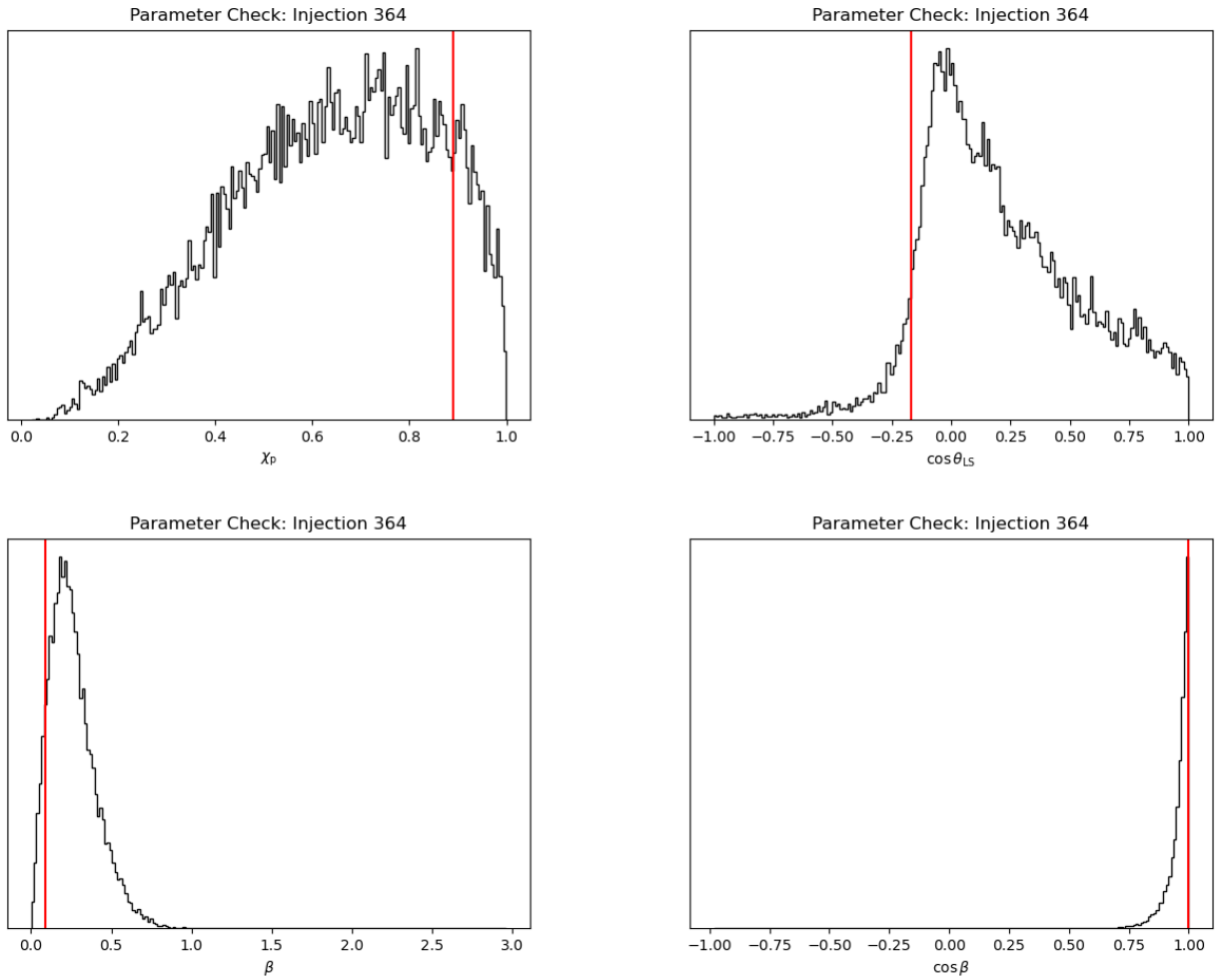

Figure 3. The posterior distributions of four parameters for a randomly selected, low-mass injection (Injection 364). Although each distribution contains the true, injected value, there are varying degrees of the breadth of each posterior distribution around the injected value. χ_p has a very broad distribution over accepted values, making it difficult to pinpoint its true value (vertical red line) without knowing it beforehand. For the same data, $\cos\theta_{LS}$ has a slightly more defined distribution around the true value. β has a narrower distribution, whereas $\cos\beta$ has the narrowest distribution of the four parameters. It is important to note that this is a general trend found across the data, but it is not necessarily the case for all posteriors. Indeed, there are some parameters in which χ_p retains a sharply defined peak in the posterior. A more quantitative value is introduced later that can statistically evaluate how good the parameter is for each injection.

Assuming that Equation (12) is approximately true, it follows that $p(d \mid \mathcal{H}_1) \approx p(d \mid \tilde{\mathcal{H}}_1)$. Using the same process as in Equations (7-10), we can express $p(d \mid \tilde{\mathcal{H}}_1)$ as

$$p(d \mid \tilde{\mathcal{H}_1}) = p(d \mid x_*, \tilde{\mathcal{H}}_1) \tag{13}$$
$$= p(d \mid x_*, \mathcal{H}_0) \tag{14}$$
$$= \frac{p(x_* \mid d, \mathcal{H}_0) p(d \mid \mathcal{H}_0)}{\pi(x_* \mid \mathcal{H}_0)}, \tag{15}$$

and plugging Equation (15) into Equation (2), we get the revised ratio

$$\Lambda = \frac{p(d \mid \tilde{\mathcal{H}}_1)}{p(d \mid \mathcal{H}_0)} \tag{16}$$
$$= \frac{\frac{p(x_* \mid d, \mathcal{H}_0) p(d \mid \mathcal{H}_0)}{\pi(x_* \mid \mathcal{H}_0)}}{p(d \mid \mathcal{H}_0)} \tag{17}$$
$$= \frac{p(x_* \mid d, \mathcal{H}_0)}{\pi(x_* \mid \mathcal{H}_0)} \tag{18}$$

This ratio, called the Savage-Dickey Ratio (SDR), provides a simpler way to compare the competing hypotheses with the use of a single parameter, allowing for a more quantitative way to evaluate the most informative parameter on the alignment of $\vec{S}_{tot}$ and $\vec{L}$.

Using the SDR, we demonstrate in Figure 4 that χ_p is not very informative about the alignment of $\vec{S}$ and $\vec{L}$, while parameters based on β (β, $\cos\beta$) are the most informative about the alignment of $\vec{S}$ and $\vec{L}$ out

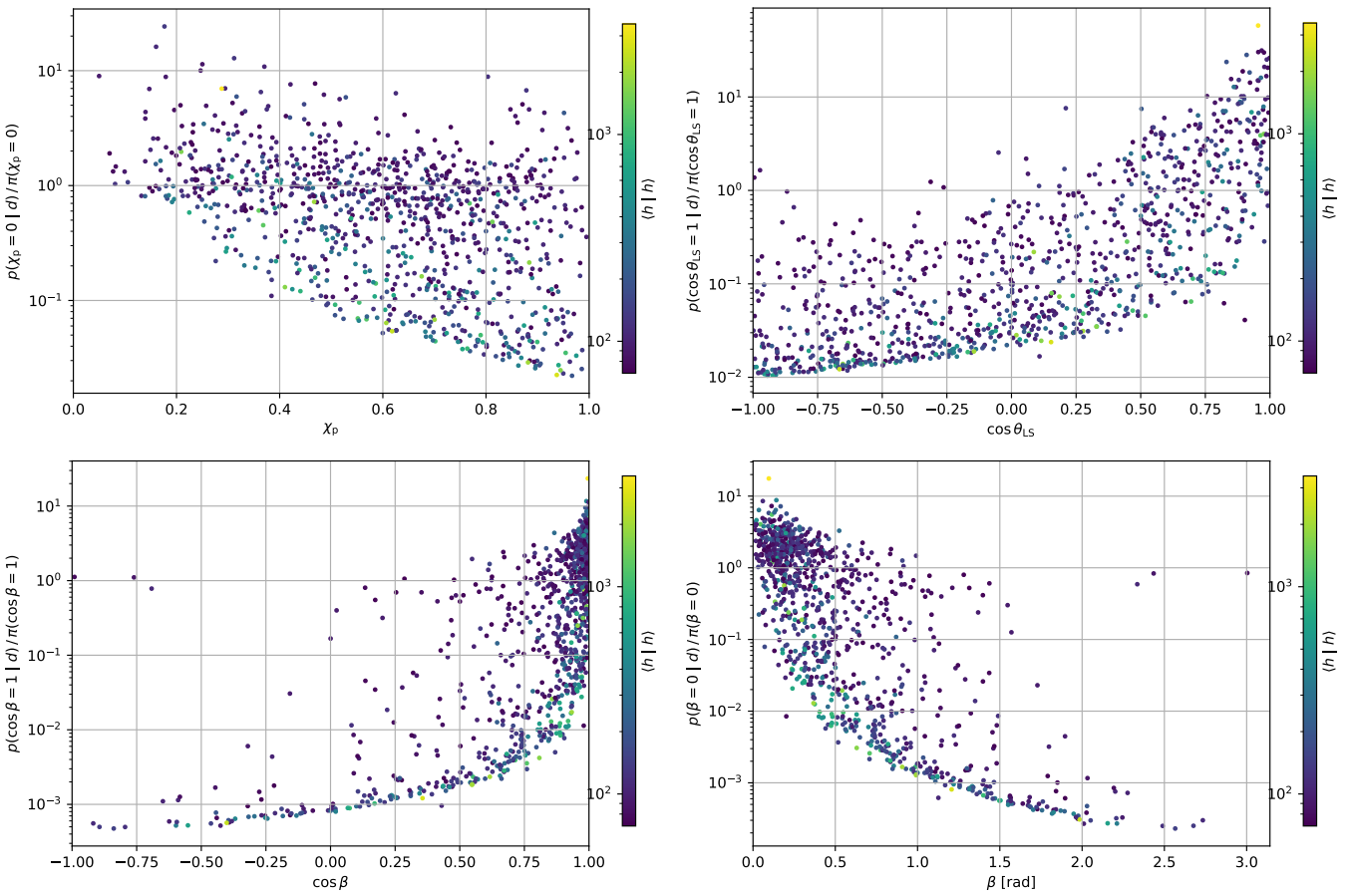

Figure 4. Savage-Dickey ratios for the three tested parameters. Each point represents an injection and associated parameter estimation. The SDR used is between the hypotheses that the spins are aligned rather than isotropic. The true, injected value is on the horizontal axis, while the Savage-Dickey ratio is on the vertical axis. The color bar symbolizes the strength of the signal h given the injected signal strength. The likelihood ratio for $\chi_{\rm p}$ is strongly clustered around values ranging from ~ 1, making it a poor test of spin alignment. Meanwhile, the likelihood ratio for $\cos\theta_{\rm LS}$ is slightly more informative. Because it spans several orders of magnitude, strongly precessing BBH systems ($\cos\theta_{\rm LS} \sim -1$) would be much more likely than weakly precessing systems to be ruled out as having aligned spins. Of the three parameters, β seems to be the most informative. The Savage-Dickey ratios that define β of the data span many orders of magnitude with a high accuracy of correctly interpreting the alignment of the spins. Generally, the SDRs for coordinate shifts of the same variable, such as from β to $\cos\beta$, should retain the same values. The slight discrepancies stem from deviations in the binned probability densities of the injection distribution.

of the three parameters tested. Currently, this analysis provides a strong incentive to evaluate the strength of the orbital precession of actual LIGO-Virgo-KAGRA sources using $\cos\beta$ as the precession parameter in place of $\chi_{\rm p}$. This is because $\cos\beta$ ($\chi_{\rm p}$) yields the highest (lowest) SDR for aligned (misaligned) spins. To choose the parameter that best defines the precession, we plan to employ another quantitative test to summarize the SDR information of each parameter in a single value.

3.1. *Comparisons to Other Spin Parameters*

Although $\chi_{\rm p}$ is currently in use as a parameter, another spin parameter, $\chi_{\rm eff}$, exists and is used to describe the mass-weighted average spin aligned with the orbital angular momentum. $\chi_{\rm eff}$ is usually much better measured that $\chi_{\rm p}$, but it provides fundamentally different information from $\chi_{\rm p}$ despite the two providing information on the spin. In order to ensure that the proposed alternative parameters to $\chi_{\rm p}$ are also providing unique information not obtained from $\chi_{\rm eff}$, we also needed to compare the SDRs of the new parameters to the likelihood ratios of $\chi_{\rm eff}$. If there is a correlation between the two, then it means that the information present in one parameter (e.g., $\cos\beta$) can also be found from $\chi_{\rm eff}$, making it less unique of a parameter. Figure 5 demonstrates that $\cos\beta$ provides unique information from $\chi_{\rm eff}$.

3.2. *Future Plans*

For the synthesized data, it appears that functions based on β (β, $\cos\beta$, and b) are able to provide a

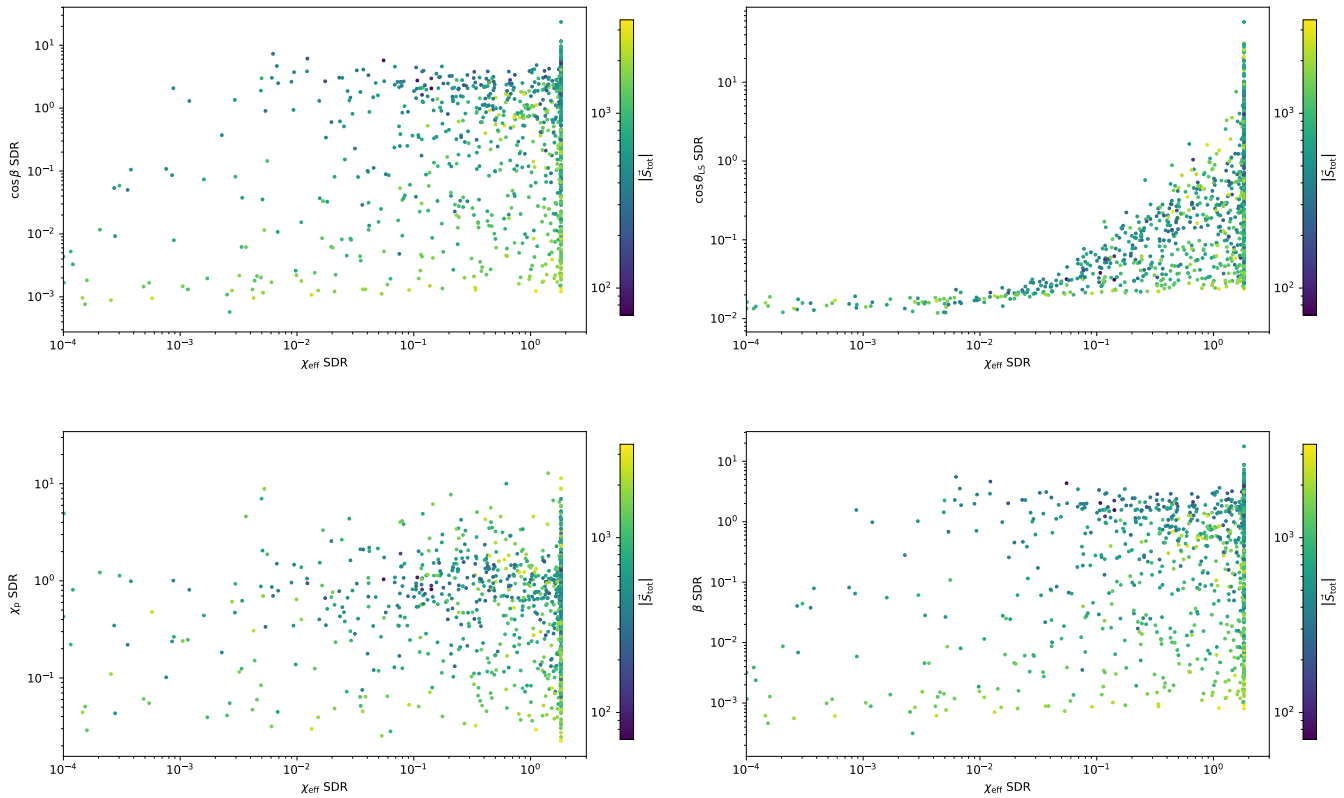

Figure 5. The Savage-Dickey ratios of the tested parameters plotted against the likelihood ratios of $\chi_{\rm eff}$ for the low-mass injections. The data are colored based on the total spin of the system. There is little correlation between the SD ratios for $\cos\beta$ and the likelihood ratios of $\chi_{\rm eff}$, meaning that the information provided from $\cos\beta$ is unique from that of $\chi_{\rm eff}$. The same is true for β (which is expected as $\cos\beta$ is a coordinate transformation of β) and for $\chi_{\rm p}$. However, given this data, $\cos\theta_{\rm LS}$ appears to be more informative than $\chi_{\rm eff}$. This is because the highest values of the SD ratio for $\cos\theta_{\rm LS}$ strongly inform the value of $\chi_{\rm eff}$, while the highest likelihood ratios for $\chi_{\rm eff}$ retain a high range of SD ratio values for $\cos\theta_{\rm LS}$. Ultimately, it appears that parameters based on β provide unique information from $\chi_{\rm eff}$, giving credence to its use as an alternative precession parameter.

stronger understanding of the angles responsible for precession than $\chi_{\rm p}$. To confirm this, we plan to devise a single value that summarizes the SDRs for each parameter to confirm which parameter is truly more informative.

Once a new parameter is chosen, the next step involves analyzing real LIGO-Virgo data from the published observing runs O1, O2, and O3 in order to re-evaluate the precession of known LIGO-Virgo sources.

4. OBSTACLES ENCOUNTERED

4.1. *Indeterminate Savage-Dickey Ratios*

One issue I encountered while running the analysis of the likelihood ratio involved the shape of the prior of $\chi_{\rm p}$ and β. For all the isotropic injections, there was not a single Savage-Dickey Ratio for β that was greater than 1 which was unexpected behavior. As both of these values approach 0 (no precession/aligned spins), the probability of the prior also approaches 0. This property makes it difficult for the SD ratio to be evaluated at 0. Using Equation (18), we can express this as

$$\lim_{\beta,\ \chi_{\rm p}\to 0} \frac{p(\text{Aligned Spins} \mid d)}{\pi(\text{Aligned Spins})} \to \frac{0}{0}. \tag{19}$$

As this expression is in indeterminate form, we can use L'Hôpital's Rule to redefine this equation as

$$\lim_{\beta,\ \chi_{\rm p}\to 0} \frac{p'(\text{Aligned Spins} \mid d)}{\pi'(\text{Aligned Spins})}. \tag{20}$$

We aimed to redefine p' and π'. We began by assuming a small area ε under the curve close to 0 for both curves (where $\varepsilon_p = \varepsilon_\pi$). Each triangle then has a base q_p and q_π. This makes the height of the triangle $h = \frac{2\varepsilon}{q}$, ultimately defining $p' = \frac{2\varepsilon}{q_p^2}$ and $\pi' = \frac{2\varepsilon}{q_\pi^2}$. The ratio of the two derivatives then is defined as

$$\frac{p'}{\pi'} = \frac{q_\pi^2}{q_p^2}. \tag{21}$$

The geometry of this derivation is outlined in Figure 6

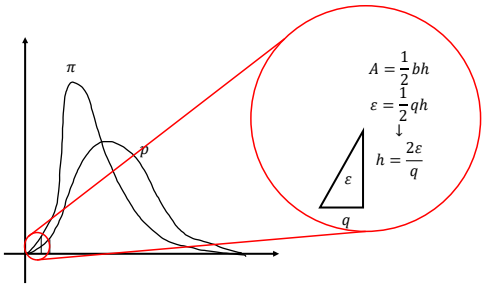

Figure 6. The geometry used to derive Equation (21).

This approach of substituting Equation (21) in for Equation (18) allowed for a much more reasonable set of SDRs for both $\chi_{\rm p}$ and β. We also tested it for several ε values ($\varepsilon = 0.003,\ 0.005,\ 0.007,\ 0.01$) and found that the shape of the resulting Savage-Dickey Ratio plots was relatively insensitive to the ε value when ε is small.

This work was supported by the National Science Foundation Research Experience for Undergraduates (NSF REU) program, the LIGO Laboratory Summer Undergraduate Research Fellowship program (NSF LIGO), and the California Institute of Technology Student-Faculty Programs.

REFERENCES

Abbott, R., Abbott, T. D., Acernese, F., et al. 2023, Physical Review X, 13, 041039, doi: 10.1103/PhysRevX.13.041039

Fairhurst, S., Green, R., Hoy, C., Hannam, M., & Muir, A. 2020, PhRvD, 102, 024055, doi: 10.1103/PhysRevD.102.024055

Hannam, M., Hoy, C., Thompson, J. E., et al. 2022, Nature, 610, 652, doi: 10.1038/s41586-022-05212-z

Mandel, I., & Farmer, A. 2022, PhR, 955, 1, doi: 10.1016/j.physrep.2022.01.003

Mehta, A. K., Olsen, S., Wadekar, D., et al. 2023, arXiv e-prints, arXiv:2311.06061, doi: 10.48550/arXiv.2311.06061

Neyman, J., & Pearson, E. S. 1933, Philosophical Transactions of the Royal Society of London Series A, 231, 289, doi: 10.1098/rsta.1933.0009

Nitz, A. H., Kumar, S., Wang, Y.-F., et al. 2023, ApJ, 946, 59, doi: 10.3847/1538-4357/aca591

Payne, E., Hourihane, S., Golomb, J., et al. 2022, PhRvD, 106, 104017, doi: 10.1103/PhysRevD.106.104017

Schmidt, P., Ohme, F., & Hannam, M. 2015, PhRvD, 91, 024043, doi: 10.1103/PhysRevD.91.024043